© EARSeL and Warsaw University, Warsaw 2005. *Proceedings of 4th EARSeL Workshop on Imaging Spectroscopy. New quality in environmental studies*. Zagajewski B., Sobczak M., Wrzesień M., (eds)

THE IMPORTANCE OF REFLECTANCE TERMINOLOGY IN IMAGING SPECTROSCOPY

Gabriela Schaepman-Strub[1], Michael Schaepman[2], Stefan Dangel[3], Thomas Painter[4], and John Martonchik[5]

1. Wageningen University, Nature Conservation and Plant Ecology, Wageningen, The Netherlands; Gabriela.Schaepman@wur.nl
2. Wageningen University, Centre for Geo-Information, Wageningen, The Netherlands; Michael.Schaepman@wur.nl
3. Univ. of Zurich, Remote Sensing Laboratories, Zurich, Switzerland; Dangel@geo.unizh.ch
4. University of Colorado, National Snow and Ice Data Centre, Boulder, USA, tpainter@nsidc.org
5. NASA, Jet Propulsion Laboratory, Pasadena, USA, John.V.Martonchik@jpl.nasa.gov

ABSTRACT

Analysing databases, field and airborne spectrometer data, modelling studies and publications, it becomes obvious, that there is a lack of consistency in definitions of reflectance quantities throughout the imaging spectroscopy user community. One example is the term 'BRDF' assigned to significantly differing quantities, ranging from the bidirectional reflectance distribution function to hemispherical-conical reflectance factors. Our contribution summarizes basic reflectance nomenclature articles. Secondly we quantify differences of reflectance products, with special emphasis on wavelength specific effects, to stress the importance of adequate usage of reflectance definitions and quantities. Results from the comparison of directional-hemispherical reflectance versus bihemispherical reflectance and bidirectional reflectance factors versus hemispherical-directional reflectance factors are shown. We exemplify differences of these quantities using modelling results of a black spruce forest canopy and snow cover, as well as biome-specific MISR reflectance products of the year 2001. The actual differences in the reflectance products of a remotely sensed surface depend on the atmospheric conditions, the surroundings, topography, and the scattering properties of the surface itself. As these effects are highly wavelength dependent, the imaging spectroscopy community has to become more specific on the application and definition of reflectance quantities. As of today most delivered reflectance products from imaging spectrometers include the hemispherical illumination component, product algorithms based on resulting at surface reflectance data have to include the actual atmospheric conditions even for nadir view angles, e.g., in the form of a wavelength specific indication of the ratio of diffuse to direct illumination. The results urge the community to treat reflectance quantities with outmost care and consistency to reduce uncertainties of derived products.

INTRODUCTION

Imaging spectrometer data and products are constantly improved in quality. Optimization is usually performed at radiance level (enhanced calibration concepts, vicarious calibration, etc.) with uncertainties approaching 4% (i), at reflectance level (atmospheric correction) with uncertainties approaching 5% (ii), at product level (sophisticated integration of various sources, assimilation, etc.) with uncertainties approaching 10% (iii), but rarely on terminology, where uncertainties can still be much higher than 10%.

The imaging spectroscopy community is developing an increased appreciation of the effects that are induced by the solar illumination and sensor viewing geometry on field, airborne and satellite data. The reflectance anisotropy of the Earth's surfaces and the atmosphere contains unique information about their structure and the optical properties of the scattering elements. The underlying concept for the characterization of the anisotropy is the bidirectional reflectance distribution func-

tion (BRDF). It describes the radiance reflected by a surface as a function of a parallel beam of incident light from a single direction into another direction of the hemisphere.

Under natural conditions, i.e. for all ground based, airborne and spaceborne sensor measurements, the assumption of a single direction of the incident beam does not hold true. Natural light is composed of a direct part, as well as a diffuse component scattered by the atmosphere, and the surroundings of the observed target. The amount and spectral character of the diffuse light irradiating the observed surface is thus depending on the atmospheric conditions, as well as on the topography and the scattering properties of the surroundings. Without correction of this diffuse component, observed reflectance quantities depend on actual atmospheric conditions, especially in the Rayleigh scattering dominated wavelength region (400-800 nm), and are not limited to the desired intrinsic directional characteristics of the observed surface. Further, the (instantaneous) field of view ((I)FOV) of the instrument most often integrates over a large viewing angle and does not allow a single beam observation. Thus, imaging spectrometer measurements do not follow the protocol of directional reflectance quantities and resulting products can only be considered as rough approximations of the surface bidirectional reflectance, a fact that is often neglected.

A physically based terminology, defining various reflectance quantities using the direction of illumination and observation, as well as their opening angle, was proposed by Nicodemus (iv), and updated by Martonchik (v). Further, recent advances originating from the Multi-angle Imaging SpectroRadiometer (MISR) science team have lead to a more uniform reflectance terminology. The operational MISR data products including different reflectance quantities are a major progress, and give users the opportunity to apply appropriate physical quantities for their investigations.

Despite above-mentioned advancements, physical conditions of measurements and corresponding terminology of at-surface reflectance quantities are still very often neglected by the user community. The loose usage of the term ‘BRDF’ is one of the most striking examples. The community performing ground based multiangular at-surface reflectance measurements often calls acquired quantities BRDF or BRF data (e.g., (vi)). But the derivation of the bidirectional reflectance distribution function (BRDF) from measurements performed under ambient sky (i.e., hemispherical) illumination results in a considerable shape distortion of the resulting function with respect to the true BRDF in the visible and near-infrared when no correction for the diffuse part of the illumination is performed, even under clear sky conditions (vii). Thus the derived so-called BRDF databases do not only reflect intrinsic bidirectional reflectance properties of the observed surface, but also wavelength-dependent effects caused by the diffuse illumination component. This is especially true for diurnal multiangular observations with changing atmospheric conditions throughout the day. Consequently, Martonchik (viii) and Lyapustin (vii) have developed methods for an accurate atmospheric correction of measured hemispherical-directional reflectance data to enhance the experimental research of anisotropic surface reflectance.

Given the confusion with and neglect of reflectance terminology as exemplified above, the aim of this paper is to summarize the basic nomenclature articles of Nicodemus (iv) and Martonchik (v) and make the updated definitions available to the imaging spectroscopy community. This overview helps to identify the correct definition for measured reflectance quantities and processed products, and to apply the appropriate quantity in physical as well as empirical approaches.

The adequate use of reflectance data does not only require a precise, widely distributed and easy to use reflectance terminology, but also an in-depth understanding of spectrodirectional effects. Therefore, the second part of the paper is aiming in demonstrating the importance of adequate use of reflectance definitions and quantities. Uncertainties, introduced by neglecting the physical basis and the corresponding terminology, are exemplified through case studies, with special emphasis on the spectral and directional domain.

This paper systematically highlights differences in at-surface reflectance quantities by their definition. We focus on the geometry of the opening angle of the illumination, i.e., directional and hemispherical extent. We quantitatively compare operational MISR directional and hemispherical reflectance products with respect to the corresponding optical depth and resulting wavelength-specific differences. Secondly, we perform a modeling exercise for forest and snow. Using a variation of

the direct to diffuse irradiance ratio in the corresponding models (i.e. RPV, DISORT), we obtain quantitative results of the wavelength-dependent influence of the diffuse component on the hemispherical-directional surface reflectance, i.e., for an illumination of hemispherical extent. We compare these results to the quantities obtained for a directional illumination only.

DEFINITIONS

Radiance, reflectance, reflectance factors

Spectral radiance is the most important quantity to be measured in spectroradiometry and is the prerequisite for the quantitative analysis of airborne and satellite measurements in the optical domain. It is the radiant flux in a beam per unit wavelength and per unit area and solid angle of that beam. It is usually expressed in the SI units [W m^{-2} sr^{-1} nm^{-1}].

Dividing the surface leaving radiance by the incident radiation onto the surface results in the so-called reflectance. Following the concept of energy conservation, the values of the reflectance are in the inclusive interval 0 to 1. The reflectance factor is the ratio of the radiant flux reflected by a surface to that reflected into the same reflected-beam geometry by an ideal (lossless) and diffuse (Lambertian) standard surface, irradiated under the same conditions. For measurement purposes, a Spectralon panel commonly approximates the ideal diffuse standard surface. Reflectance factors may reach values beyond 1, especially for highly specular reflecting surfaces.

The reflectance factor, adapted to the remote sensing problem and respecting particular directional issues, can generally be defined as follows, using the notations in Table 1:

$$R(\theta_i, \phi_i, \omega_i; \theta_r, \phi_r, \omega_r; \lambda),$$

where the direction and the solid angle of the circular cone of the incoming and the reflected radiance are indicated. A refinement of this definition leads to the following special cases:

- ω_i or ω_r are omitted when either is zero (directional quantities).
- If 0 < (ω_i or ω_r) < 2π, then θ, ϕ describe the direction of the centre axis of the cone (e.g. the line from a sensor to the centre of its ground field of view).
- If $\omega_i = 2\pi$, the angles θ, ϕ indicate the direction of the incoming direct radiation (e.g., the position of the sun). However, for remote sensing applications, it is often useful to separate the natural incoming radiation into a direct and hemispherical diffuse part. The preferred notation for the geometry of the incoming radiation is then $\theta_i, \phi_i, 2\pi$, thus keeping the position of the sun. It must be noted that in this case, θ_i, ϕ_i do not describe the centre of the cone (2π), except if the sun's position is at nadir.
- If $\omega_r = 2\pi$, θ_r and ϕ_r are omitted.

According to Nicodemus (iv), abbreviations for resulting reflectance quantities name the angular characteristics of the incoming radiance first in the term, followed by the angular characteristics of the reflected radiance. This leads to the attributes of spectrodirectional reflectance quantities as illustrated in Table 2.

Table 1: Notations used for the definition of at-surface reflectance quantities.

Symbol	Explanation
ρ	reflectance [dimensionless]
R	reflectance factor [dimensionless]
θ	zenith angle, in a spherical coordinate system [rad]
ϕ	azimuth angle, in a spherical coordinate system [rad]
ω	solid angle $\equiv \int d\omega \equiv \iint \sin\theta \cdot d\theta \cdot d\phi$ [sr]
λ	wavelength of the radiation [nm]
f()	function
sub- and superscripts	
i	incident
r	reflected

Table 2: Relation of incoming and reflected radiance terminology used to describe reflectance, with mathematical description of commonly used quantities (see Figure 1 for abbreviations). The labelling with 'Case' corresponds to Nicodemus (iv). Grey fields correspond to measurable quantities, whereas the others denote conceptual quantities.

Incoming/ **Reflected**	**Directional**	**Conical**	**Hemispherical**
Directional	Bidirectional Case 1 $BRDF = f_r(\theta_i, \phi_i; \theta_r, \phi_r; \lambda)[sr^{-1}]$ $BRF = R(\theta_i, \phi_i; \theta_r, \phi_r; \lambda)$ 	Directional-conical Case 2 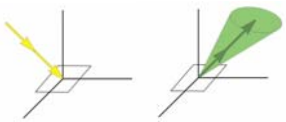	Directional-hemispherical Case 3 $DHR = \rho(\theta_i, \phi_i; 2\pi; \lambda)$ 
Conical	Conical-directional Case 4 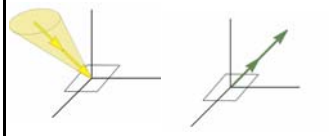	Biconical Case 5 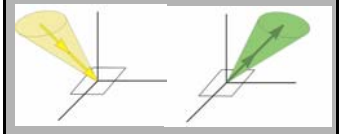	Conical-hemispherical Case 6 
Hemispherical	Hemispherical-directional Case 7 $HDRF = R(\theta_i, \phi_i, 2\pi; \theta_r, \phi_r; \lambda)$ 	Hemispherical-conical Case 8 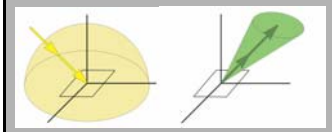	Bihemispherical Case 9 $BHR = \rho(\theta_i, \phi_i, 2\pi; 2\pi; \lambda)$ 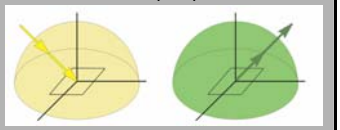

Conceptual and measurable reflectance quantities

From a physical point of view, there is the possibility to define special cases, namely conceptual and measurable reflectance quantities. Conceptual quantities of reflectance include the assumption that the size/ distance ratio of the illuminating source (usually the sun or lamp) and the observing sensor is zero. They are usually labeled *directional* in the general terminology. Since infinitesi-

mal elements of solid angle do not include measurable amounts of radiant flux, and unlimited small light sources and sensor FOVs do not exist, all measurable quantities of reflectance are performed in the *conical* or *hemispherical* domain of geometrical considerations. Thus, actual measurements always involve non-zero intervals of direction and the underlying basic quantity for all radiance and reflectance measurements is the conical case. The integration of the reflected radiance over a solid angle corresponds e.g. to the opening angle of the sensor. Under field conditions, the incident radiance cone is of hemispherical extent ($\omega = 2\pi$ [sr]). The irradiance can then be divided into a direct sunlight component and a second irradiance component, which is scattered by the atmosphere, the terrain, and surrounding objects, resulting in an anisotropic, diffuse sky illumination. Being a function of wavelength, the ratio of diffuse/direct irradiance highly influences the spectral dependence of directional effects as shown in the quantitative case studies.

Referring to Table 2, the most common measurement setup of satellites, airborne and field instruments corresponds to the hemispherical-conical configuration (Case 8) (e.g., MERIS, ASD FieldSpec). Albedometers approximate the bihemispherical configuration (Case 9). Finally, a typical laboratory setup corresponds to the biconical configuration (Case 5), where a collimated light source illuminates a target that is measured using a non-imaging spectroradiometer (e.g., EGO (Koechler, 1994), and LAGOS (Dangel, 2003)). The non-zero interval of the sensor's instantaneous field of view may be neglected for small opening angles and resulting quantities are then reported as bidirectional (laboratory measurements) or hemispherical-directional (small IFOV ground based, airborne, and spaceborne measurements).

Processing of reflectance quantities

Figure 1 shows the derivation of different reflectance products from satellite data, as implemented in the MISR processing scheme (ix). The integration of the at-surface HDRF (Case 7) over the viewing hemisphere results in the BHR (Case 9). Using a modelling approach (e.g., (vii), (viii), (ix)), the HDRF data (Case 7) are further used to derive BRF (Case 1), and finally, DHR (Case 3) can be derived from BRF (Case1) by hemispherical integration over the viewing hemisphere.

The multiangular measurement configuration of MISR allows for the presented derivation of different reflectance products, using consistent terminology. For many other satellite and airborne systems, the user community is faced with products simply called 'surface reflectance', a term not allowing the assignment of the corresponding illumination conditions (i.e., directional or hemispherical) without further knowledge on the preprocessing and corresponding beam geometries. As a consequence, these data are subject to misinterpretation, and subsequently their uncertainties increase.

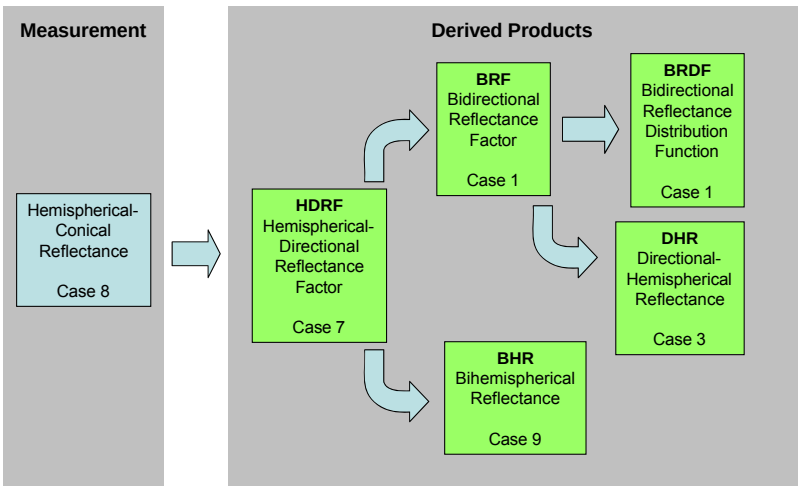

Figure 1: Conceptual data processing chain of airborne and satellite measurements to convert a reflectance measurement (Case 8) into BHR, BRDF, and DHR, as implemented in the MISR processing scheme.

CASE STUDIES ILLUSTRATING DIFFERENCES OF REFLECTANCE QUANTITIES

The following case studies highlight differences of the described reflectance quantities using A) MISR data products for several selected biome types, as well as model simulations for B) a vegetation canopy, and C) snow cover. The differences of hemispherical versus directional reflectance and reflectance factors (i.e., BHR (Case 9) versus DHR (Case 3) and HDRF (Case 7) versus BRF (Case1)) are computed for the visible to shortwave infrared wavelength range, and different ratios of direct to diffuse illumination conditions.

The analysis of MISR data highlights differences of reflectance quantities including data, algorithm and model uncertainties, as well as wavelength dependent aerosol optical depth values. Thus it reveals expectable differences of real satellite data products, whereas the two simulation studies emphasize on general features of different reflectance quantities for vegetation and snow.

A) Analysis of MISR surface reflectance data products

Various land surface reflectance products are available from the MISR sensor, launched in 1999. MISR has nine cameras with centre view directions of 26.1, 45.6, 60.0, and 70.5 degrees in forward and afterward direction, as well as one looking in nadir direction, all covering four spectral bands with a centre wavelength at 446, 558, 672, and 867 nm (x).

For the retrieval of the reflectance products please refer to (9). We statistically analyzed the differences of directional and hemispherical MISR reflectance data products, namely DHR versus BHR and BRF versus HDRF. These data products are compared to each other by their respective mean values, mean absolute and relative difference, and their correlation. Further, the mean aerosol optical depth (AOD) value in the green spectral band of all analyzed pixels was calculated.

The ratio of diffuse to direct illumination increases with increasing AOD. Therefore we expect the largest difference between HDRFs and BRFs in shorter wavelength ranges, i.e., in the blue band, where the diffuse component of the illumination is largest. This wavelength dependence is due to the decreasing influences of Rayleigh scattering and aerosols with increasing wavelength.

We selected ten datasets, acquired in 2001, corresponding to MISR data product version 12. The reliability of the land surface reflectance values depends upon the AOD magnitude. Therefore, pixels with an AOD larger 0.5 at 558 nm (green spectral band) were excluded from the MISR scenes. The sites were selected to represent different biome types, following the MODIS IGBP land cover map (Table 3).

Table 3: Overview of MISR scenes selected for the analysis of the land surface products.

Site	Date 2001	SZ [°]	AOD	IGBP Biome
Howland, Maine, US	07/21	27.7	0.10	Mixed forests, deciduous broadleaf forests, evergreen needleleaf forests
Railroad Valley, Nevada, US	08/17	28.4	0.10	Open shrublands, grasslands, woody savannas
Mongu, Zambia	07/11	44.6	0.05	Savannas, cropland/ natural vegetation mosaic, woody savannas, grasslands
Banizoumbou, Niger	10/04	24.1	0.31	Open shrublands, grasslands, savannas
	12/23	41.4	0.11	
Hombori, Mali	07/05	19.6	0.36	Open shrublands, barren or sparsely vegetated, grasslands
Avignon	07/12	25.2	0.07	Croplands, mixed forest, water bodies
	08/29	36.9	0.19	
Bordeaux	05/30	24.5	0.24	Evergreen needleleaf forests, croplands, cropland/ natural vegetation mosaic, woody savannas, mixed forests
	07/01	24.0	0.12	

In general, BHR (Case 9) and DHR (Case 3) product values derived from the MISR sensor are highly correlated, with r^2 values between 0.98 and 1.0 throughout all spectral bands and analyzed

scenes (with the exception of the Hombori scene blue band, where r^2 reaches 0.84 only). For all analyzed MISR images, the relative scene-averaged difference between BHR and DHR reaches a maximum of 2.7 % of the BHR value (with the exception of the difference in the blue band of the Hombori scene reaching 5.1%) for all four spectral bands (Table 4). We expect a trend of decreasing differences between BHR and DHR with increasing wavelength, thus largest relative differences in blue band reflectances. This proves to be right for 5 cases, whereas for the other 5 cases, differences reach the same or even higher values in at least one of the other bands. Differences between the BHR and DHR product can be related to the actual aerosol optical depth in the green spectral band. This relation is weak for the BHR-DHR differences in the blue band (r^2 = 0.29) and gets much stronger with increasing wavelengths, with a maximum for the NIR region (r^2 = 0.79).

As with the results for the hemispherical reflectances, the relationship between HDRF (Case 7) and BRF (Case 1) values show a high correlation, with r^2 values above 0.98 throughout all spectral bands, and view angles of all scenes (the Hombori scene blue band reflectance reaching an r^2 of 0.67 only). Compared to the quantities integrated over an extrapolation of the view hemisphere, the relative differences of the reflectances of the single view angles are larger and reach up to 10% of the HDRF value (the Hombori scene blue band with a reflectance difference of 14.2%). The trend of decreasing differences with increasing wavelength is much stronger for the directional quantities than for the hemispherically integrated quantities. Thus, the largest relative differences were mostly found in the blue spectral band. Comparing the relative HDRF-BRF differences with regard to the viewing direction, there is a clear trend of higher differences for the forward looking camera. Further we investigated the relative differences of the HDRF-BRF values with regard to the nine cameras. For most scenes and spectral bands, the Ba camera (view zenith of 45.6º) shows the smallest differences.

Table 4: Comparison of BHR and DHR values for the selected MISR scenes.

Site	SZ [°]	AOD 558nm	Mean BHR/ Mean((BHR-DHR)/BHR) [%]			
			446nm	558nm	672nm	867nm
Howland	27.7	0.10	0.031/ 2.1	0.053/ 1.5	0.028/ 1.1	0.318/ 0.7
Railroad Valley	28.4	0.10	0.095/ 1.7	0.137/ 1.3	0.170/ 0.9	0.238/ 0.7
Mongu	44.6	0.05	0.046/ 0.5	0.078/ 0.3	0.094/ 0.3	0.246/ 0.6
Banizoumbou	24.1	0.31	0.060/ 1.2	0.126/ 1.5	0.176/ 1.4	0.357/ 1.3
	41.4	0.11	0.084/ 0.5	0.160/ 0.5	0.261/ 0.6	0.376/ 0.6
Hombori	19.6	0.36	0.108/ 5.1	0.232/ 2.5	0.349/ 1.6	0.412/ 1.2
Avignon	25.2	0.07	0.045/ 2.0	0.075/ 1.4	0.069/ 0.9	0.307/ 0.8
	36.9	0.19	0.050/ 0.9	0.081/ 0.9	0.079/ 0.7	0.286/ 0.8
Bordeaux	24.5	0.24	0.059/ 1.5	0.097/ 2.0	0.087/ 1.4	0.320/ 1.2
	24.0	0.12	0.048/ 1.8	0.078/ 1.5	0.073/ 1.0	0.304/ 0.9

B) Vegetation canopy reflectance simulations using the RPV model

Using the PARABOLA instrument, black spruce forest HDRF data were observed at eight solar zenith angles (35.1º, 40.2º, 45.2º, 50.2º, 55.0º, 59.5º, 65.0º, 70.0º) (xi). After applying a simple HDRF to BRF atmospheric correction (xii), data of the red spectral band (650 - 670 nm) were fitted to the parametric Rahman-Pinty-Verstraete (RPV) model (xiii). Resulting fit parameters and the RPV model were used to simulate different reflectance quantities of a black spruce canopy under various illumination conditions. The model was run for a solar zenith angle of 30° and increments of direct (*d*) and diffuse irradiance of *d* = 1.0, 0.8, 0.6, 0.4, 0.2, 0.0. These irradiance scenarios correspond to BRF for *d* = 1.0, and HDRF for the rest.

As expected for a vegetation canopy, backscattering is the dominating reflectance feature for the black spruce BRF data, with a pronounced hot spot at a view zenith of 30° (Figure 2, 3). Adding an isotropic diffuse irradiance component results in HDRF data. With decreasing direct irradiance, the anisotropy is smoothed. Finally, the hot spot disappears for a scenario based on diffuse irradiance only. Concentrating on nadir view data, the relative difference between the bidirectional and the

hemispherical-directional reflectance factor can be significant, especially for illumination zenith angles around solar noon, approaching the hot spot configuration (Figure 3). Even though absolute differences between single BRF and HDRF data are numerically small for the selected wavelength range and certain geometries, it becomes obvious that BRDF functions can strongly be distorted, when derived from model fits based on HDRF instead of BRF data.

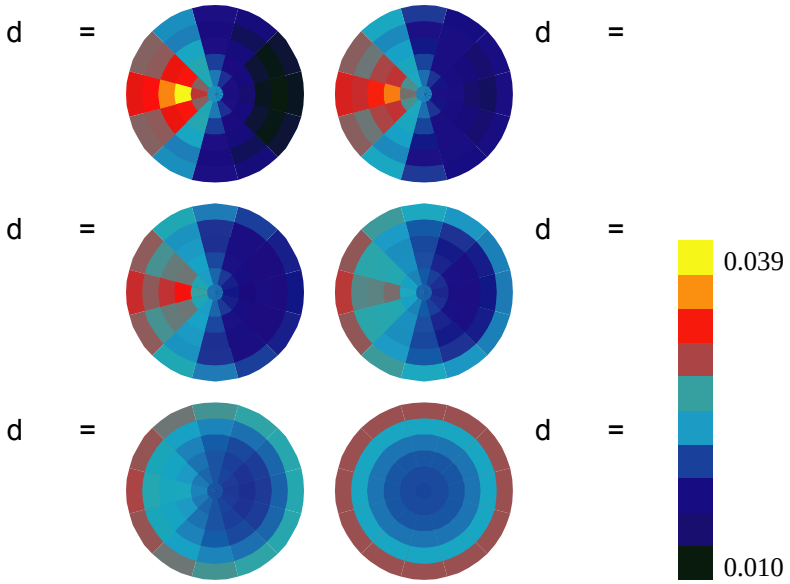

Figure 2: Reflectance factors of a black spruce forest canopy at 650-670 nm as a function of view angle. The direct illumination, at 30° zenith, is from the left. The six plots illustrate the influence of the relative amount of direct illumination. The top left image corresponds to pure direct irradiation, thus to BRF data, all others to HDRF data (from d = 0.8 to d = 0). The bottom right image corresponds to totally diffuse irradiation (d = 0).

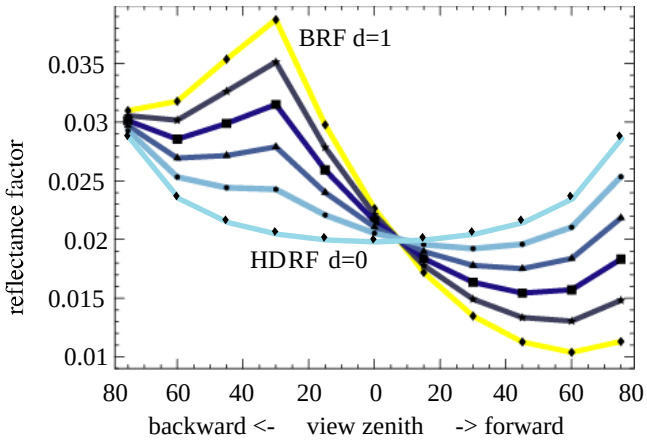

Figure 3: Simulated BRF (d=1.0) data for a black spruce canopy in the solar principal plane, and corresponding HDRF for varying direct to diffuse irradiance conditions (d=0.8 to d=0.0).

C) Snow reflectance simulations

This case study presents results from snow directional reflectance simulations, coupling single-scattering parameters and the discrete-ordinates multiple scattering model DISORT (xiv). The single-scattering parameters used in the model were the single-scattering albedo, extinction efficiency, and the single-scattering phase function, determined with a ray-tracing approach for spheroidal particles (xv). Simulation results correspond to a spheroid of minimum and maximum radii of 208 μm and 520 μm, respectively. We then determined 20 Legendre moments of the single-scattering phase function for input to the multiple scattering model. The multiple scattering model

was run for a solar zenith angle of 30° and increments of direct (*d*) and diffuse irradiance of *d* = 1.0, 0.8, 0.6, 0.4, 0.2, and 0.0.

In Figure 4, we show the angular distributions of the irradiance scenarios for wavelength 0.55 μm. The models for *d* = 1.0 through *d* = 0.2 exhibit a forward reflectance distribution that decreases in magnitude with increasing diffuse component. For the totally diffuse irradiance scenario, the distribution shows a shallow bowl shape. This minimum at nadir results from the angular intersection of the strong forward scattering phase function with the surface. Off-zenith irradiance has a greater chance than zenith irradiance of surviving multiple scatterings due to the orders of magnitude greater single scattering in the forward direction. In other words, zenith irradiance requires far more scattering events to produce reflected radiance than off-zenith. Therefore, the distribution shows greater reflectance at larger view zenith angles. The solar principal plane for these scenarios is given in Figure 5 (top). The bowl-shaped distribution in the principle plane for diffuse irradiance becomes relatively deeper at longer wavelengths (Figure 5 (bottom)), such as 1.03 μm. We show the 1.03 μm model because this is the wavelength range in which snow reflectance is most sensitive to grain size (xvi). The enhancement of the bowl shape at greater diffuse irradiance is explained as above coupled with a decrease in the single-scattering albedo at the longer wavelengths. Only for the BRF and *d* = 0.8 irradiance cases is the distribution properly forward reflecting.

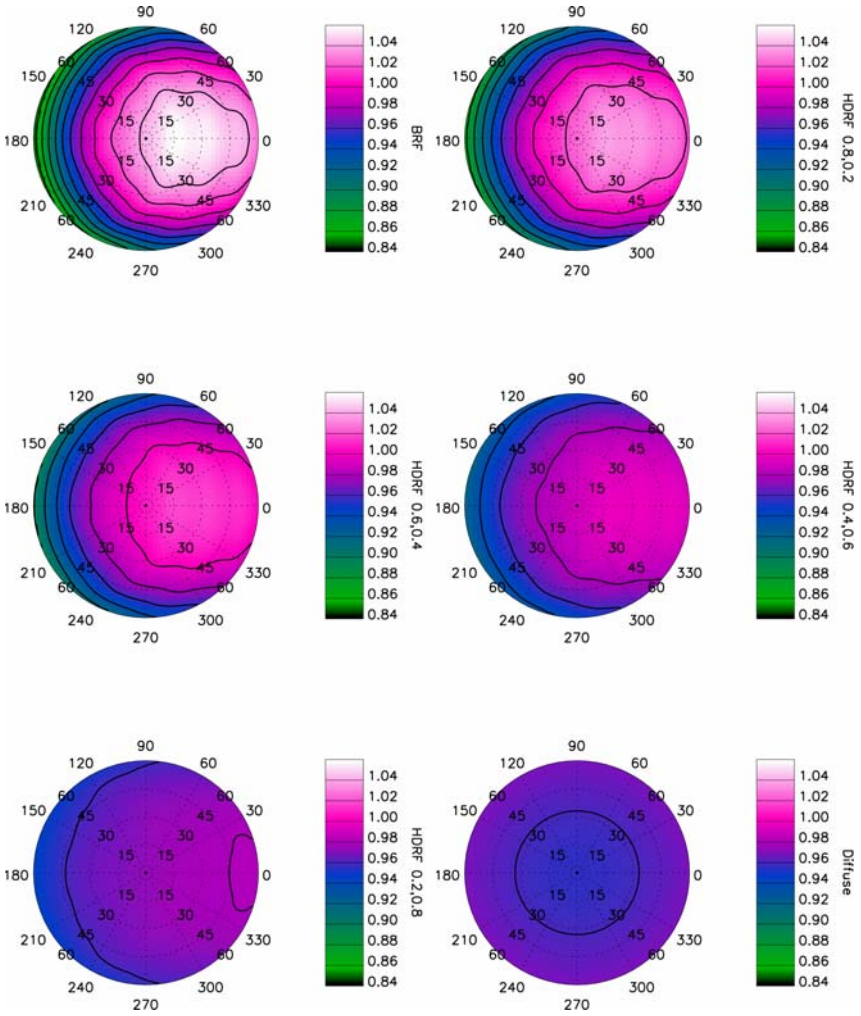

Figure 4: Angular distributions of reflectance for a range of irradiance cases at 0.55 µm and solar zenith angle = 30°. The target centre represents the nadir view geometry θ_r, ϕ_r = (0°, 0°), radial distance from centre represents the view zenith angle, and the angle about the centre represents the view azimuth angle. The forward reflectance direction is ϕ_r = 0°.

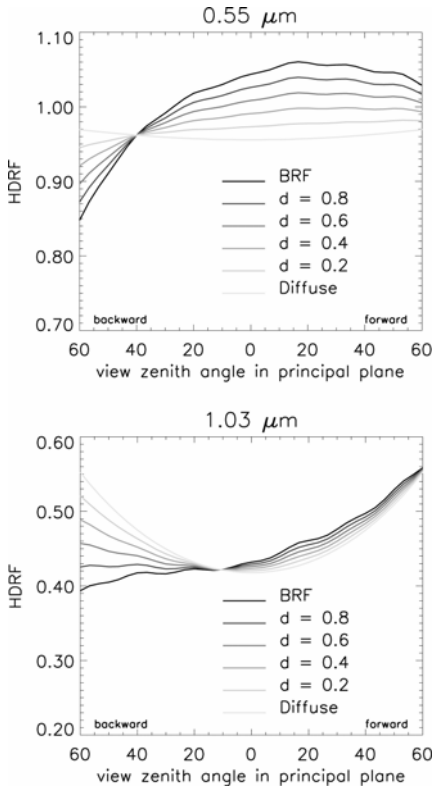

Figure 5: Directional reflectance in the principal plane for a range of irradiance scenarios at wavelengths 0.55 µm (top) and 1.03 µm (bottom).

CONCLUSIONS

All remote sensing data depend on the illumination and view geometry of the sensor, as well as on their opening angle. Different reflectance quantities have been defined to describe the corresponding conditions of the measurements. The basis for the proper use of these reflectance quantities is a standardized nomenclature, well known throughout the remote sensing community. This study summarized the nomenclature articles of Nicodemus (iv) and Martonchik (v) to give an easy access to the concept. Further the importance of using the adequate reflectance in product is shown. All reflectance measurements performed under natural conditions include a diffuse fraction, which is a function of the atmospheric conditions, the topography, the surroundings of the observed surface, and the wavelength. It thus introduces spectral effects into spectrometer data. The presented case studies are concentrating on the opening angle of the illumination. The effect of varying direct to diffuse irradiance ratio is significant in modelled data, as well as in analysed MISR reflectance products. This study is especially addressing the imaging spectroscopy community, due to the wavelength dependence of the shown effects. It shows the importance of including the corresponding illumination and view geometry, and the opening angle in definitions and analysis. Thus, any analysis of uncorrected spectrometer data has to account for wavelength dependent effects introduced by the diffuse irradiance, which are not intrinsic spectral signatures of the observed scene. In modelling exercises, the diffuse irradiance has to be considered, and eventually be accounted for by indicating the direct/diffuse irradiance fraction wavelength dependently. This study highlights that the presented nomenclature is not only important for multiangular data sets, but also for the characterisation of the irradiance of any remotely sensed reflectance data. Therefore, the publication shall motivate the imaging spectroscopy community to take reflectance nomenclature into account and use the presented common basis for clarity and comparability of data and results.

ACKNOWLEDGEMENTS

This work was supported by the Swiss National Science Foundation, under contract 200020-101517 and through an SNF fellowship grant for prospective researchers. The MISR data were obtained from the NASA Langley Research Center, Atmospheric Sciences Data Center.

REFERENCES

i Fox N, J Aiken, J J Barnett, X Briottet, R Carvell, C Frohlich, S B Groom, O Hagolle, J D Haigh, H H Kieffer, J Lean, D B Pollock, T Quinn, M C W Sandford, M Schaepman, K P Shine, W K Schmutz, P M Teillet, K J Thome, M M Verstraete, & E Zalewski, 2003. Traceable radiometry underpinning terrestrial- and helio-studies (TRUTHS). Advances in Space Research, 32: 2253-2261

ii Kneubühler M, M E Schaepman, K J Thome, & D R Schläpfer, 2003. MERIS/ENVISAT vicarious calibration over land. In: Sensors, Systems, and Next-Generation Satellites VII, edited by R Meynart, S P Neeck, H Shimoda, J B Lurie & M L Aten (SPIE, Barcelona), Vol. 5234, 614-623

iii Rast M, F Baret, B van de Hurk, W Knorr, W Mauser, M Menenti, J Miller, J Moreno, M E Schaepman & M Verstraete, 2004. SPECTRA - Surface Processes and Ecosystem Changes Through Response Analysis (ESA Publications Division, Noordwijk), ESA SP-1279(2)

iv Nicodemus F, J Richmond, J Hsia, I Ginsberg & T. Limperis, 1977. Geometrical Considerations and Nomenclature for Reflectance (NBS, US Department of Commerce, Washington, D.C)

v Martonchik J, C Bruegge, & A Strahler, 2000. A review of reflectance nomenclature used in remote sensing. Remote Sensing Reviews, 19: 9-20

vi Schonermark M, B Geiger & H P Roeser, 2004. Reflection Properties of Vegetation and Soil (Wissenschaft und Technik Verlag, Berlin) 352 pp.

vii Lyapustin A I & J L Privette, 1999. A new method of retrieving surface bidirectional reflectance from ground measurements: Atmospheric sensitivity study. Journal of Geophysical Research-Atmospheres, 104 (D6): 6257-6268

viii Martonchik J, 1994. Retrieval of Surface Directional Reflectance Properties Using Ground-Level Multiangle Measurements. Remote Sensing of Environonment, 50 (3): 303-316

ix Martonchik J V, D J Diner, B Pinty, M M Verstraete, R B Myneni, Y Knyazikhin & H R Gordon, 1998. Determination of land and ocean reflective, radiative, and biophysical properties using multiangle imaging. Ieee Transactions on Geoscience and Remote Sensing, 36 (4): 1266-1281

x Diner D, J Martonchik, C Borel, S Gerstl, H Gordon, Y Knyazikhin, R Myneni, B Pinty, M Verstraete, 1999. Multi-angle Imaging Spectro-Radiometer Level 2 Surface Retrieval Algorithm Theoretical Basis (JPL, California Institute of Technology) JPL D-11401, Rev. D, December 2, 1999

xi Deering D W, S P Ahmad, T F Eck & B P Banerjee, 1995. Temporal Attributes of the Bidirectional Reflectance for three Boreal forest canopies. In: IGARSS (Florence, Italy), 1239-1241

xii Tanre D, M Herman & P Y Deschamps, 1983. Influence of the Atmosphere on Space Measurements of Directional Properties. Applied Optics, 22 (5): 733-741

xiii Engelsen O, B Pinty, M Verstraete & J V Martonchik, 1996. Parametric bidirectional reflectance factor models: evaluation, improvements and applications (EC Joint Research Centre, Ispra, Italy), 114 pp.

xiv Stamnes K, S C Tsay, W Wiscombe & K Jayaweera, 1988. Numerically Stable Algorithm for Discrete-Ordinate-Method Radiative-Transfer in Multiple-Scattering and Emitting Layered Media. Applied Optics, 27 (12): 2502-2509

xv Macke A & M I Mishchenko, 1996. Applicability of regular particle shapes in light scattering calculations for atmospheric ice particles. Applied Optics, 35 (21): 4291-4296

xvi Nolin A W & J. Dozier, 2000. A hyperspectral method for remotely sensing the grain size of snow. Remote Sensing of Environment, 74 (2): 207-216